IEEE Open Access Journal of
Power and Energy

Received 15 September 2022; revised 7 January 2023; accepted 8 January 2023. Date of publication 26 January 2023;
date of current version 24 May 2023.

Digital Object Identifier 10.1109/OAJPE.2023.3239854

Telephone Interference From Solar PV Switching

GAURAV SINGH[1] (Member, IEEE), THOMAS COOKE[1] (Member, IEEE), JASON JOHNS[1] (Member, IEEE), LUIS VEGA[2] (Member, IEEE), ARIEL VALDEZ[2] (Member, IEEE), AND GLORIA BULL[2] (Member, IEEE)

[1]Power Quality Research Group, Electric Power Research Institute, Knoxville, TN 37932 USA
[2]Dominion Energy, Richmond, VA 23219 USA

CORRESPONDING AUTHOR: G. SINGH (gsingh@epri.com)

This work was supported by Dominion Energy, Richmond, VA, USA.

ABSTRACT The emergence of solar Photovoltaic (PV) generation has been one of the biggest changes in the Power Grid in the past decade. Such generation plants are generally inverter based and these devices are known sources of harmonics of the fundamental frequency and 'supraharmonics' (distortion in the frequency range **2** to **150 kHz**). It has long been theorized that due to factors such as the frequency response of service transformers that interface solar PV plants to the grid, impedance of the power system at the point of common coupling and the impedance of devices connected near solar inverters, supraharmonics frequencies are localized and generally do not couple to the grid. Exceptions to this general hypothesis have been reported in Europe, where supraharmonics from PV and wind power plants have been shown to couple to the local three-phase three wire Medium Voltage (MV) system. This paper shows that in three-phase four wire multi-point grounded MV systems, such as the ones used in the United States (U.S.), application of conventional grounding schemes to PV plants can lead to the unintended consequence of coupling of supraharmonics to the grid through the neutral conductor and ground circuit. It describes a case study in which supraharmonics due to inverter switching led to telephone interference for customers located around a solar PV plant. To determine the mechanism by which the supraharmonics frequencies were coupling to the grid, an investigation of the emission from the plant was performed using conducted as well as radiated measurements. The novel setup used for performing these radiated measurements, the unique underlying mechanism by which inverter switching frequencies coupled to the grid and the lessons learned in this process regarding solar PV grounding and installation practices are described in this paper.

INDEX TERMS Supraharmonics, solar, interference, telephone, noise.

I. INTRODUCTION

THE emergence of renewable, low-carbon energy resources such as solar PV has been one of the biggest developments in the power sector in the past decade. Presently, an increasingly large amount of solar PV plants are being integrated into the power system, all around the world. Solar PV plants generally tend to utilize inverters, which are known sources of harmonics of the fundamental frequency (< 2 kHz) and supraharmonics (2 to 150 kHz) distortion. Due to these emission characteristics, there has justifiably been some worry on the part of Power Quality (PQ) engineers about increasing grid compatibility problems, as PV plants proliferate [1]. In the harmonics frequency range, standards such as IEEE 519 [2] and IEC 61000-3-2 [3] lay down limits on the maximum allowable distortion in the system. However, such regulations do not extend into the supraharmonics frequency range where emission components due to high speed power electronic switching tend to dominate. This, however, is not entirely problematic. Early research has indicated that supraharmonics generally tend to be localized, in large part because at the supraharmonics frequencies, devices connected near a source of supraharmonics offer a lower impedance path, as opposed to the grid [4], [5], [6], [7]. A case study presented in CIGRE Technical Brochure 799 [8] supports this observation in regards to PV inverters by showing that inverter supraharmonic emission is more likely

to flow between inverters than into the grid. A further layer of isolation between the grid and sources of supraharmonics is provided by the service transformer. It has been shown in [9] for example that a Medium Voltage (MV) to Low Voltage (LV) service transformer provides a fair degree of damping for supraharmonics being injected into the MV system from the LV system. This means that the magnitude of supraharmonic distortion is typically reduced when propagating from the LV connected load to the MV network. The exception to this observation are frequencies that occur near the transformer's resonant points. Further research and PQ measurements have shown, however, that these observations and theories are not applicable under all circumstances or to be taken as general rules. For example, PQ recordings and case studies from Europe have shown that renewable energy resources are a dominant source of supraharmonics in the MV grid [10], [11], [12]. The power electronic inverters that are used to interface such generating resources to the grid inject harmonics and supraharmonics into the MV grid while injecting active and reactive power into the grid [13]. This injection of harmonics and supraharmonics depends upon the grid impedance at the Point of Common Coupling (PCC), transfer impedances in the grid and its resonance characteristics and has been extensively discussed in [14] through the use of a case study from Sweden. In addition to renewable energy resources, [15] further shows a case study indicating that supraharmonics distortion from datacenters can also couple to the MV grid.

The preceding discussion showed that although supraharmonics tend to be localized, they can couple to the upstream MV grid from the LV side in a three-phase three wire MV system. This paper shows that in three-phase four wire multipoint neutral grounded systems such as the ones found in the U.S., a further exception to this rule exists, and that supraharmonics can actually propagate to the MV system through the ground network and the neutral conductor. It supports this assertion by detailing a case study from the U.S. where switching frequencies from a PV plant propagated into the MV grid and caused interference with the telephone system in the surroundings. The rest of this paper presents the background of the case study and the investigation that followed. Conclusions from the work and recommendations for design changes and installation practices are presented in the final few sections of this work.

II. BACKGROUND

In January 2021, utility PQ engineers responded to a problem of Electromagnetic Interference (EMI) that was occurring in the vicinity of three solar PV plants in the United States. Customers near the PV plants had been complaining of unusually high audible background noise from the Plain Old Telephone Service (POTS) that they used in their homes. The electric utility was keen to identify the root cause of the problem quickly and implement corrective actions such as changes in design and commissioning philosophy, so that a recurrence of the problem could be avoided. To identify the interfering

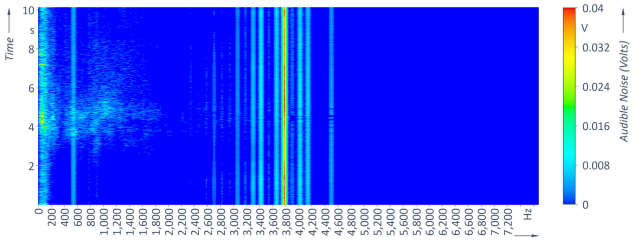

FIGURE 1. Spectrum of audio recording from a customer site. Frequency is on the x-axis while Time is plotted on the left y-axis. The plot shows relative RMS magnitude of frequencies in the audio file in units of volts.

frequencies, audio recordings of the background noise being heard by the affected customers, were first made. The frequency spectrum of one such audio recording is shown in Fig. 1. This figure shows the spectrum of voltage provided as output by the microphone used to record the audio signal and shows that the spectrum contained a dominant component at 3.78 kHz and other sidebands between 2.5 kHz and 4.5 kHz. The dominant component of 3.78 kHz corresponded to the switching frequency of the inverters at the nearby solar PV plant. Similar investigations at the other two sites further confirmed that the audible noise being heard by the customers in those cases, was also caused by switching of the solar PV inverters. IEEE 519 [2], quantifies such telephone interference using the Telephone Interference Factor (TIF) which depends upon the amplitude of a spectral component as well as its frequency (some frequencies have higher impact on interference than others), with components between 2 and 3.3 kHz having the highest impact. Thus, even though the 3.78 kHz component in the spectrum shown in Fig. 1 has the highest amplitude, it is likely and probable that all frequency components in the spectrum had a part to play in this audible background noise.

While the analysis of the audio recordings confirmed the correlation of audible background noise with PV inverter switching, the larger question of how these inverter switching frequencies coupled to the local telephone system remained unanswered. Furthermore, early attempts to alleviate the problem by implementing inverter firmware changes only succeeded at two of the three affected plants (the reasons for why two of these sites were successful in alleviating this problem are discussed later in this paper). In order to find the coupling mechanism by which the switching frequencies were propagating to the MV grid and to understand why firmware changes were only a partial success, the utility approached EPRI and a joint project to investigate the EMI issue was launched. To narrow the focus of the investigation, the plant where inverter firmware changes had failed to alleviate the problem was selected (coincidentally, this was the same plant that caused the background noise spectrum shown in Fig. 1). Having selected the site, the next step in this investigation was a comprehensive review of the electrical design of the solar plant and that of the nearby POTS lines. The findings of this design review stage are explained next.

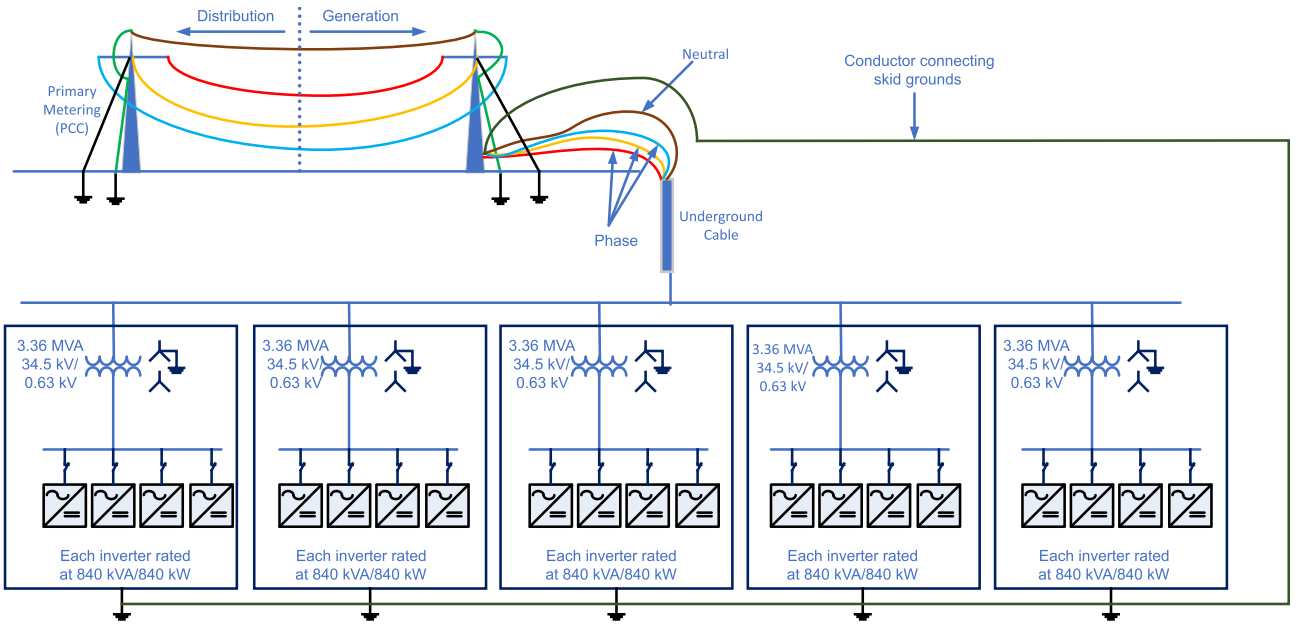

FIGURE 2. Simplified schematic diagram of the solar PV plant.

III. DESIGN REVIEW

A. SOLAR PLANT

The solar PV plant selected for this investigation was located on the East Coast of the United States and had an installed capacity of about 17 MVA. A simplified schematic diagram of the layout of this plant is shown in Fig. 2. This schematic shows that the solar plant consists of five individual stations where four inverters and a step-up transformer are present. Each such 'station' is referred to as a 'skid'. The skids are distributed over a very large geographical area, with an average distance of at least 90 m between individual skids. A skid is the heart of the operation and converts the DC power provided by the solar panels into usable AC at the MV distribution level.

1) SOLAR PV INVERTERS

Each inverter at the PV plant was rated at 840 kW at a power factor of unity (effectively 840 kVA). Each skid consisted of four such inverters and hence, the skid had a rated power handling capacity of 3.36 MVA. The switching frequency of each inverter was 3.78 kHz. Time domain waveforms of the voltage generated by these inverters, and a spectrum of an individual phase are shown in Fig. 3. These waveforms were measured at the primary metering point of the solar plant (refer to Fig. 2) and are influenced by the frequency response of the step-up transformer (as opposed to being measured directly at the output of the inverter). The Potential Transformers (PTs) used for these measurements measured the Line-to-Ground voltage at the metering point which had a value of 20 kV nominal. The PT's had a ratio of 175 : 1 and therefore the RMS value of the measured primary signal that they produced had a magnitude of 114 V. The measurements

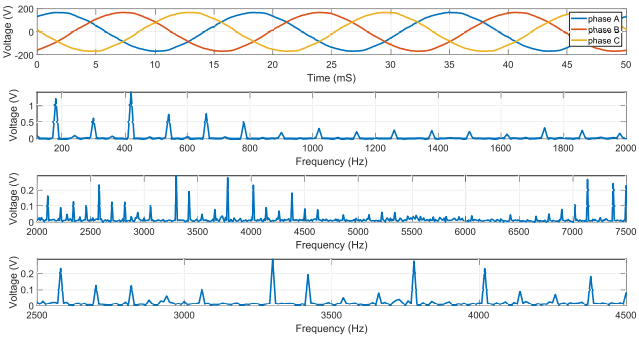

FIGURE 3. Time domain waveforms of the voltage produced by the solar PV plant (top). Spectrum of phase A voltage is shown separately in the frequency range up to 2 kHz (second from top) and 2 kHz to 7.5 kHz (third from top). A zoomed in view of the switching frequency of the inverter and its residue in the frequency range 2.5 kHz to 4.5 kHz is shown at the bottom.

were made by a PQ monitor sampling the input signals at a rate of 256 samples per cycle. The time domain waveforms in Fig. 3 show some minor distortion near the peak of the waveform but show little influence of harmonic distortion from visual inspection. The spectrum of voltage, on the other hand, displays a rather interesting behavior and offers insight into a possible reason for the failure of inverter firmware changes in alleviating the EMI problem. The spectrum of inverter voltage shows odd harmonics of the power frequency up to 2 kHz, which are characteristic of the front ends of power electronic circuits. In addition, it also shows frequency components beyond 2 kHz and all the way up to about 4.5 kHz, including the switching frequency and its side bands (the same spectral components as seen in Fig. 1). Inverter

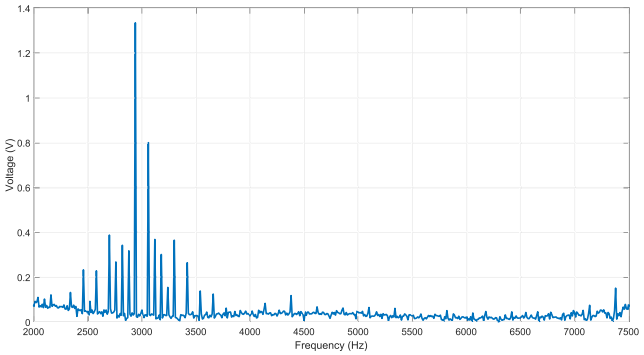

FIGURE 4. Spectrum of phase A voltage from a solar plant in the supraharmonics frequency range, where phase cancellation of supraharmonics alleviated the background noise issue.

firmware changes typically involve changing the phase angle at which the switching frequency components are emitted, so that individual inverters produce these components out of phase with each other, leading to phasor cancellation. In this case, however, the number of frequency components produced by inverter switching is rather large and it can be seen that producing phasor cancellation of all these components would be difficult. Further, as noted in the previous section, each of these switching frequency components was likely to produce interference with the telephone system and selectively eliminating just a few frequencies would not alleviate the problem either. To bring out this point further, Fig. 4 shows the spectrum of emission in the voltage of another solar plant where inverter firmware changes did alleviate the audible noise (Note that this voltage was measured with the same instrumentation as described previously and the same PT ratios and sampling speed apply. The difference in magnitude of the frequency components between the two inverters is likely caused by the time of day at which these measurements were made). Fig. 4 shows that in the PV plants where inverter firmware changes did alleviate the issue (the plants used a different make and model of inverter), a sharply defined emission at a switching frequency of 3 kHz and some sidebands, was observed from the inverter. Compared to the case of Fig. 3, it can be seen that the inverter switching produces less 'residue' (i.e., less frequency components) in the frequency domain, allowing for the possibility of eliminating the switching frequency and its sidebands by having pairs of inverters be phase-shifted from each other i.e., the emission from a pair of inverters is phase shifted so that they cancel the emission from each other. Although it could not be said with complete certainty, it is possible that this difference in emission character was the reason for firmware changes proving ineffective at the one PV plant.

2) INVERTER STEP UP TRANSFORMER

The other major component of the PV plant that affected its emission was the inverter step up transformer. In the PV plant studied, each skid was provided with a transformer with a rated capacity of 3.36 MVA. The transformer had an impedance of 5.75% and stepped up the voltage provided by the inverter from 630 V to the distribution system voltage of 34.5 kV. Each transformer had an ungrounded wye-grounded wye configuration. The inverters were connected to the ungrounded wye windings while the grounded wye side was connected to the distribution system.

3) CONDUCTORS AND ASSOCIATED INFRASTRUCTURE

The last major piece of the solar plant was the layout of the conductors. At the PV plant, the generated power was carried from the five skids to a riser pole just outside the premises, by a cable with a concentric neutral wire. As shown in Fig. 2, the plant had two riser poles adjacent to each other, with the pole at which the cable conductors and neutral wire were brought out, belonging to the Generating company, and the adjacent pole belonging to the Distribution company. The Point of Common Coupling was the primary metering point and located on the Distribution company's pole. In addition to the three phase and (one) neutral conductors, the plant also had a fifth conductor (shown in green color in Fig. 2). Outside each skid, a copper rod was driven into the ground and this rod provided the ground reference for each skid. This fifth conductor, referred to as the 'skid ground' conductor connected these five copper rods together and back to the generation neutral which was, in turn, grounded. The skid ground conductor was likely used to provide a zero sequence current reference to the protection system, and for the control circuits inside the skids. It was later discovered that this conductor had a role to play in carrying the switching frequency current from the skids to the Distribution system. The investigation leading up to the discovery of the root cause, implicating this grounding system is explained next.

IV. INVESTIGATION AND MEASUREMENT

A. RADIATED EMISSIONS MEASUREMENT

Having reviewed the solar PV plant design in some detail, the next step was to investigate possible mechanisms by which EMI could result between the plant and the POTS lines. These POTS lines ran parallel to the solar PV plant, about 10 m from its boundary and at least 150 m from the nearest skid (refer to Fig. 8). Generally, EMI problems arise due to conducted emission, but in cases investigated by the authors, emission radiated by solar PV plants has also been known to cause such issues [16]. In order to investigate this possibility of radiated emission from the solar PV plant interfering with the POTS lines, measurements of the radiated emission were made inside the solar PV plant and in the vicinity of the POTS lines. These measurements had the following two goals:

- To measure the emission being radiated by components inside the solar plant and whether these levels were sufficient to couple with the distribution system and induce switching frequency distortion in the voltage.
- To measure the distance to which the emission from the solar plant was being radiated and to quantify the

probability that the radiated emission was directly interfering with the nearby POTS lines.

1) MEASUREMENT EQUIPMENT

Solar PV plants have many parts that can produce radiated emission and hence the area to be covered for such measurements is quite large. Manual surveys and measurements are therefore difficult and time-consuming. EPRI engineers have developed novel solutions to overcome this issue and detect and quantify radiated emissions. Two such solutions are the EPRI robotic platform known as the 'Big Autonomous Mobile Measurement Platform (BAMMP)' and an EPRI-developed mobile platform for measuring radiated emissions and baselining them, known as the 'Portable Radiated Emission Measurement System', or 'PREMS II'. The BAMMP was utilized to measure the levels of emission inside the plant while the PREMS II was used to measure the levels of radiated emission near the POTS lines.

The BAMMP is a robotic platform capable of acquiring highly accurate and repeatable measurements using a wide variety of sensor instrumentation. Autonomous localization and navigation are provided using on-board light detection and ranging (LIDAR) and global positioning system (GPS) sensors. The LIDAR additionally allows for mapping of indoor spaces, where GPS is not available. From these two sensors, localization data can then be combined with other measurements, such as: temperature and humidity, light spectrum, electromagnetic interference (EMI) spectrum, electric field, radiation and nuclide, and air quality. A photograph of the BAMMP is shown in Fig. 5.

FIGURE 5. Photograph of the BAMMP platform.

In order to characterize the radiated emission from solar PV plant components, the BAMMP was fitted with a Tektronix RSA306 spectrum analyzer, which is capable of measurements between 9 kHz and 6.2 GHz. Since this spectrum analyzer could not scan below 9 kHz, it had a conspicuous incapability to scan for the inverter switching frequencies. To overcome this shortcoming, a second spectrum analyzer, namely the Aaronia Spectran NF-5035, was utilized. The scan range on this spectrum analyzer was set to 1 kHz to 20 kHz, so that the full range of frequencies emitted by the solar PV inverters could be covered between the two spectrum analyzers. With this measurement capability, sites could be evaluated for interference problems. The procedure involved measurement of multiple sites inside the PV plant, with a frequency scan performed at each site. A heat map of the measured radiation, at each individual measurement frequency was then prepared.

Whereas the BAMMP focused on the measurement and characterization of radiated emissions inside the solar PV plant, emissions measurement outside the plant were carried out using the PREMS II. The PREMS II is a second-generation EPRI-developed system that carries out electromagnetic field measurements using the same spectrum analyzers as the BAMMP. As compared to the BAMMP, however, the PREMS II had a higher degree of portability because it can be manually transported in the bed of a truck or a similar vehicle. An example of such an arrangement is shown in Fig. 6, where the PREMS II apparatus is mounted in the bed of an All Terrain Vehicle (ATV).

FIGURE 6. Example of the EPRI PREMS II system mounted in the bed of an ATV.

Using a specialized computer, measurements of radiated emissions can be geographically coordinated using GPS coordinates. Using the PREMS II, measurements of radiated electromagnetic fields along the neighborhood of the POTS lines were taken, to determine whether the inverter switching frequencies propagated as far as the locations of the POTS lines. Similar to the outcome of measurements using the BAMMP, the results of the wide-area survey using the PREMS II were displayed as a heat map of the radiated emission in the vicinity of the POTS lines. An example of such a heat map is shown in Fig. 7. Apart from radiated emissions from the solar PV plant itself, there were suspicions that there may be

some conducted propagation of switching frequencies from the solar PV plant to transmission lines (Fig. 3 shows that such conducted propagation did indeed happen as inverter switching frequencies can be detected at the PCC), which may then get radiated into the surroundings. This wide-area survey included measurement of any such radiation from transmission lines. A summary of the results of these measurements, showing the results from inside and outside the plant on a single consolidated heat map, are presented next.

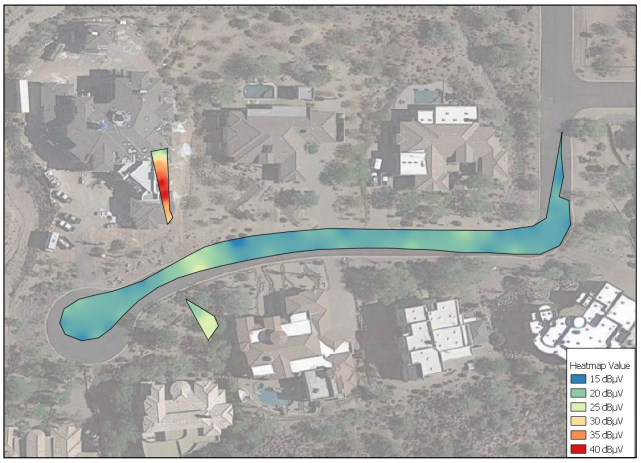

FIGURE 7. Example of a heat map generated from a wide-area survey performed using the EPRI PREMS II at a frequency of 12.5 kHz.

2) SUMMARY OF RADIATED MEASUREMENTS

Using the measurement apparatus previously described, heat maps of the emission radiated by the solar plant were created. Although separate measurement platforms were used to measure the levels of radiated emission inside and outside the plant, the results were ultimately plotted on the same heat map. One such heat map, overlaid on a satellite map of the solar plant and quantifying the radiated emission levels at 3.3 kHz, in and around the solar plant is shown in Fig. 8. Due to the limited frequency resolution of the measurement equipment, the emission at the switching frequency of 3.78 kHz could not be captured. However, as the spectrum of emission from the PV inverter has shown, the inverter produces quite a bit of switching residue. In fact, Fig. 3 shows that the inverter produces a slightly higher emission component at 3.3 kHz than at the switching frequency of 3.78 kHz. Fig. 8 shows that at this frequency, about 10 to 30 dB μV of emission is observed at the POTS lines. To get an understanding of how much attenuation this represents, it is useful to look at the emission from the source i.e., the solar PV inverters. This is shown in Fig. 9 which shows the emission levels around skid 2 in the plant. This heat map shows that around the skid, the radiated emission is significantly high, in the range of about 50 to 70 dB μV. However, as the distance from the inverter increases, the radiated emission gets damped very quickly. As Fig. 9 shows, even at distances of about 10 to 15 m, the decibel value of radiated emission gets attenuated by two to three times. It is worth noting that skid number 5 was located about 100 m from the POTS lines (see Fig. 8). However, as seen in Fig. 9, the radiated energy from the inverter gets damped very quickly and this distance was enough for most of the radiated energy to be effectively attenuated at the POTS lines.

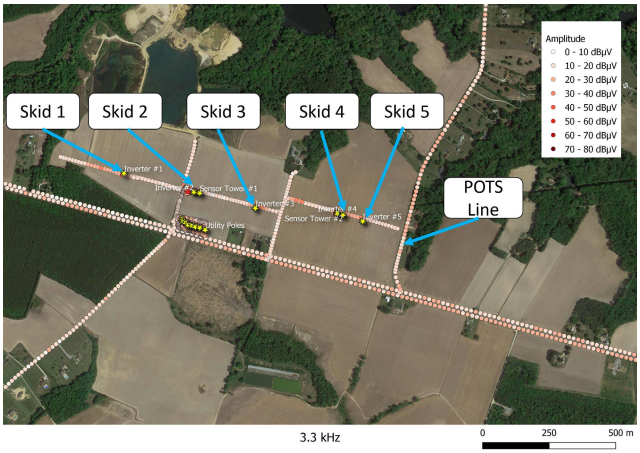

FIGURE 8. Heat map showing levels of radiated emission in and around the solar plant at a frequency of 3.3 kHz.

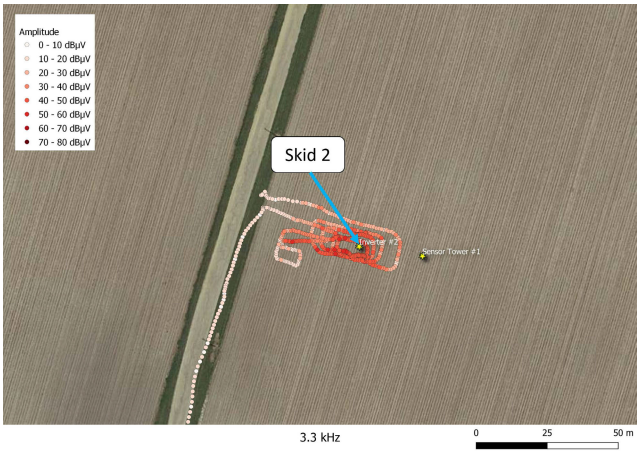

FIGURE 9. Heat map showing levels of radiated emission near skid number 2 at the solar plant at a frequency of 3.3 kHz.

Fig. 8 showed that near the POTS lines, about 10 to 30 dB μV of radiated emission at 3.3 kHz was recorded. This value was about 5 dB μV lower than the level which produced Amplitude Modulation (AM) radio interference from a solar plant in a previous study of radiated emission [16]. In addition to this slightly lower value (lower than the level which would likely produce interference) of radiated emission near the POTS line, there was another important factor which indicated that radiation was likely not the mechanism via which switching frequencies were interfering with the

POTS lines. The POTS lines were essentially copper cables buried under the ground. This one factor, coupled with the rapid attenuation of radiated energy from the inverter gave an indication that in all likelihood, radiated emission could be eliminated as the source of coupling between the POTS lines and the solar PV plant. This indicated that the inverter switching frequencies were being conducted to the POTS lines.

The list of useful inferences that could be drawn from the radiated emissions benchmarking of the solar PV plant did not end with just the elimination of radiation as a possible coupling mechanism. The radiated emissions measurement actually provided a vital clue about how the switching residue of the inverter was propagating to the distribution system. To understand this point, it is useful to look at the heat map of the solar PV plant at 9 kHz. This frequency represents the lower scanning limit or the starting frequency of the Tektronix spectrum analyzer used in the radiated emissions measurements. This heat map is shown in Fig. 10.

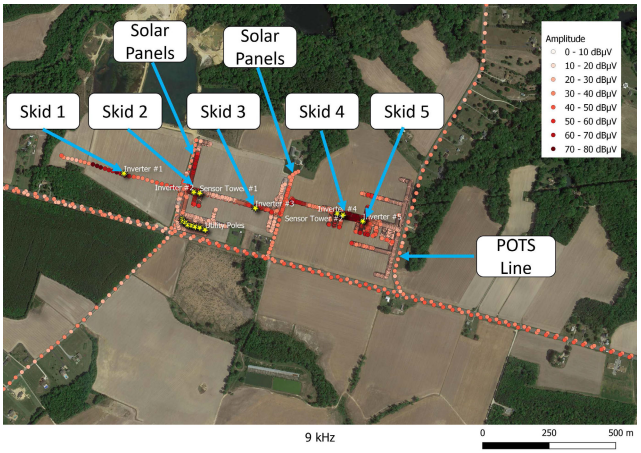

FIGURE 10. Heat map showing levels of radiated emission at 9 kHz in and around the solar PV plant.

A comparison of Fig. 8 which shows radiated emission at 3.3 kHz, and Fig. 10 indicates a higher level of radiated emission from the solar plant at 9 kHz than at 3.3 kHz. What is even more interesting is that the rate at which this radiated emission attenuates with distance, is a lot lower than the emission at 3.3 kHz. This can be further verified by examining the radiated emission inside the plant near a skid. This has been shown for skid number 2 in Fig. 11. Near the inverter, the radiated emission at 9 kHz has a magnitude between 60 and 80 dB μV. Near the solar panels, this radiated emission level is between 50 and 70 dB μV. This behavior is quite different to the one seen at 3.3 kHz where the radiated emission attenuates rather quickly with distance. The only logical explanation for this observation is that the 9 kHz frequency must be present in conducted form at the panels and is being radiated either by a conductor or by a conducting surface. This assertion was further verified through conducted emissions measurements which are described later in this paper. The other important question of why the radiated emission at 9 kHz is higher than at 3.3 kHz can be attributed to or explained on the basis of a resonant frequency in the solar plant circuit. This resonant point is likely being excited by the switching residue from the inverters, leading to the 9 kHz radiated emission being higher in magnitude.

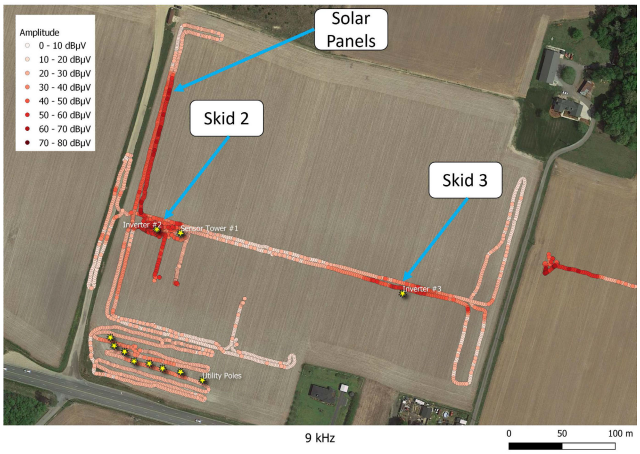

FIGURE 11. Heat map showing levels of radiated emission at 9 kHz near skid number 2 at the solar PV plant.

The conclusion that the 9 kHz frequency is being radiated near the solar panels is rather unexpected in of itself. The solar panels convert solar energy into electricity and provide it to the solar inverters in the form of DC current. In such a case, it is highly unlikely that the conductors (two conductors of positive and negative polarity) carrying current from the panels would have any high frequency AC present. One possible explanation that makes engineering sense, for the presence of the 9 kHz frequency at the solar panels was that the third conductor i.e., the grounding conductor running from the solar panels to the junction boxes to the inverters, must carry this frequency. In order to confirm this theory, two tasks were therefore undertaken:

1) A detailed study of the grounding at the solar plant was undertaken. Design documents from the plant were thoroughly reviewed and analyzed in this process. Furthermore, a detailed literature review was undertaken to see if similar cases had been documented elsewhere.
2) Measurements of the conducted emission at the solar plant were undertaken. These measurements especially emphasized measurements of the currents and voltages associated with the plant grounding circuit.

These studies and measurements confirmed the theory that the ground circuit at the solar PV plant was indeed carrying switching frequency current and this circuit led to the coupling of such frequencies to the distribution system, and in turn the POTS system. The mechanism by which the switching frequencies couple to the grounding circuit and the analyzes which led to the confirmation of the ground network being the source of coupling between the solar PV plant and the POTS lines are detailed next.

B. CONDUCTED EMISSIONS ASSESSMENT

1) GROUNDING DESIGN REVIEW

The previous section showed that the radiated emissions measurement eliminated the possibility of radiated Electromagnetic Interference with the POTS lines. In addition, the radiated emissions also indicated that the ground network of the solar plant may be potentially involved in the EMI problem. In order to understand the involvement of the grounding system in the EMI issue and to investigate the other possibility, of conducted interference, a review of the electrical connections of the POTS system was first performed, followed by conducted emissions measurement. The POTS system generally receives power from a source independent of the local power grid, minimizing the chances of interference between them. A review of the grounding connections of the POTS lines, however, revealed a possible link between the distribution system and the POTS system. A schematic diagram of the POTS lines, in relation to the distribution system is shown in Fig. 12. The POTS lines are essentially shielded copper cables. Fig. 12 shows that the shielding on these cables is bonded to the same point at which the neutral wire in the local four wire distribution system is grounded. Further investigation revealed that this is a common practice and at each point at which a given distribution pole is grounded, the local POTS line is bonded to this grounding point. In other words, if the inverter switching frequencies were to couple via the distribution system neutral conductor, they would have more than a single point available to couple with the telephone system in the area. To verify this hypothesis of conducted coupling through the neutral-ground network, however, measurements of the current flowing in the distribution system neutral wire were necessary. These measurements, and an analysis of the grounding of the PV plant are therefore presented next.

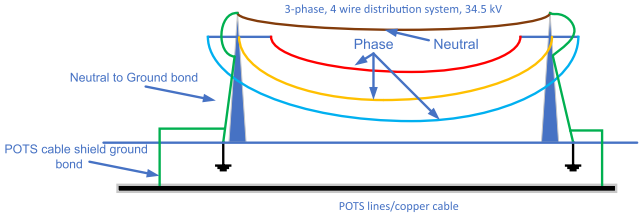

FIGURE 12. Schematic diagram of the POTS lines and their grounding.

2) ANALYSIS AND MEASUREMENTS OF THE GROUND CIRCUIT

The previous section showed that an electrical link between the distribution system and the telephone system existed through the ground network. This observation, and the further lack of any connection between the two systems suggested that the coupling of switching frequencies to the telephone system must happen on the neutral-ground network. To confirm this hypothesis, an experiment was conducted. The data from this experiment (and all conducted measurements shown hereafter) was collected using a Dewetron DEWE3-A4 portable data acquisition system operating at a sampling speed of 200 kHz. The voltages were measured directly using this system without the use of differential voltage probes. Current measurements on the other hand, were performed using Pearson model 8590C current probes. These probes have a transfer of 1 V/ A and an accuracy of $\pm 1\%$ in the frequency range of interest. In this experiment, all the skids at the PV plant were sequentially shut down, while simultaneously the audible noise on the telephone system was observed. Further to this, the current flowing in the telephone cable's grounding conductor was measured. The spectra of this current in two operating conditions: one with one skid operating at the PV plant and another with the whole plant shut down, are shown in Fig. 13. This figure shows that with the inverters in operation, the current in the telephone cable grounding conductor contained a high amount (16 mA at switching frequency) of inverter switching frequency and its sidebands. However, as soon as the last inverter was turned off, these spectral components corresponding to inverter switching disappeared. At the same time, a reduction in the background noise being heard on the telephone lines was observed.

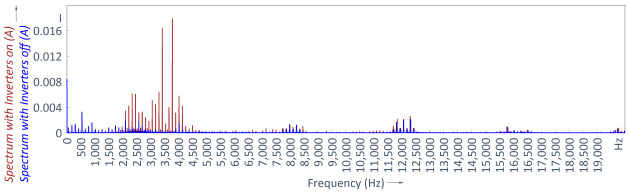

FIGURE 13. Current in the POTS cable grounding conductor with one skid on (red) and all inverters off (blue).

Fig. 13 provides proof that the inverter switching frequencies coupled to the telephone lines through the ground circuit. A re-examination of Fig. 3 provides further confirmation of this hypothesis. In this figure, the spectrum of phase voltage (measured line to neutral) is presented. This voltage was measured on the transformer's MV side at a voltage of 34.5 kV and shows supraharmonics frequencies. As [9] has shown, supraharmonic frequencies are generally damped while coupling through a transformer's LV winding to its MV winding. Hence, one possible source for supraharmonics in this voltage could be common mode noise in the neutral wire. This information further suggests that the neutral wire could carry switching frequency current from the solar plant and into the system. The next question to consider in the investigation was the conditions under which switching frequencies would flow on the distribution system neutral wire and into the ground network. Fig. 2 shows that the distribution system neutral conductor was connected to three conductors at the generation company's pole. These three conductors were: 1. The concentric neutral coming from the PV plant, connecting the transformer MV winding neutrals together, 2. The skid ground conductor and 3. The generation

company's pole ground. Additionally, the system neutral was also grounded at each subsequent distribution pole, including the distribution company pole shown in Fig. 2. The presence of switching frequency current in any of these conductors would likely lead to the flow of this current in the system neutral, subsequently leading to its coupling with the POTS lines. To identify which of these conductors contributes to this flow of switching frequency current in the neutral wire, an experiment was set up. In this experiment, the current in the distribution system neutral wire was monitored, while the concentric neutral conductor and the skid ground conductor were sequentially disconnected from the circuit (the solar plant was operating 'as intended' in this experiment i.e., all inverters were online and generating). With these conductors removed, the solar plant and the distribution system effectively operated without a ground reference and were in a 'floating' condition. The spectra of currents from this experiment are shown in Fig. 14. The top plot in this figure shows the spectrum of current in the neutral wire when the plant is operating as intended i.e., with all conductors connected as prescribed. With the concentric neutral conductor removed (second plot), the switching frequency components and their sidebands reduced by about 30%. Further, in the next step (third plot), when the skid ground conductor was removed, an additional 60% reduction in components associated with inverter switching was seen. Finally, the figure also shows a condition with all inverters offline. This experiment showed that the switching frequency current actually flowed in both, the concentric neutral conductor as well as the skid ground conductor. About a third of the switching frequency supraharmonic current flowed in the concentric neutral while about two-thirds flowed in the skid ground conductor. As a final point, it is worth pointing out that when the supraharmonics frequencies are unable to reach the system neutral conductor due to the concentric neutral and the skid ground conductor being removed, energy at the supraharmonics frequencies flows to the distribution company pole through the earth to the pole ground. This can be observed from Fig. 15, which shows measurements of the earth voltage between the generation and distribution company poles. As the paths to the system neutral wire were successively removed, it was seen that the earth voltage between the poles increased (due to increased current flow in the earth), confirming that the neutral-ground circuit was involved in the propagation of the supraharmonics frequencies.

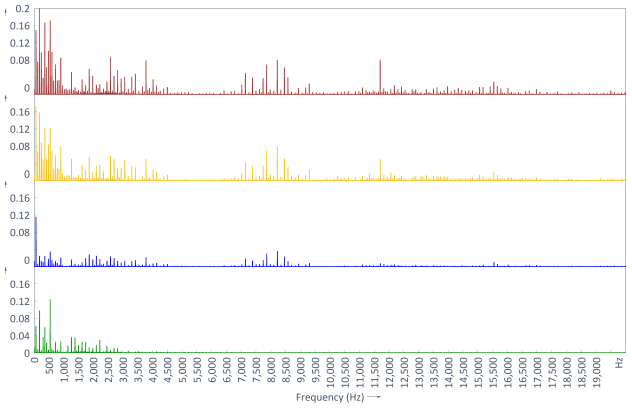

FIGURE 14. Spectra of neutral current in normal operation (top), with the concentric neutral removed (second from top), with the PV plant floating (third from top) and with all inverters offline (bottom). All currents are in Ampere (A).

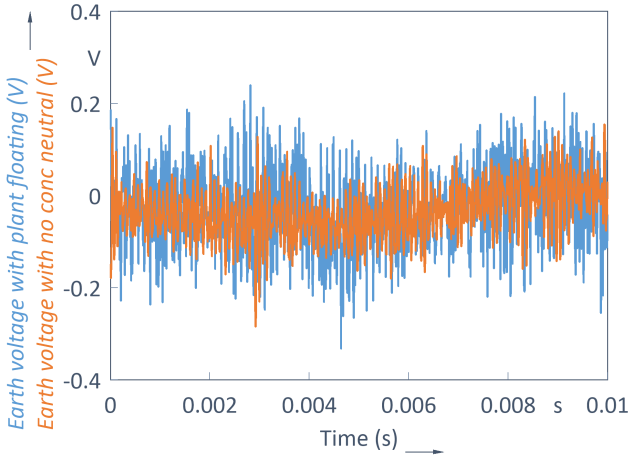

FIGURE 15. Pole to pole earth voltage with the concentric neutral removed (red) and with the PV plant floating (blue).

C. ORIGIN AND PROPAGATION OF SWITCHING FREQUENCY CURRENT

The previous sections showed that switching frequency current coupled to the system neutral through the concentric neutral wire and the skid ground conductor. Since neither of these conductors is directly connected to the inverters in any discernible way, it naturally leads to questions about the origin of the supraharmonics current in these conductors. The use of an ungrounded winding on the LV side of the transformer implies that such frequencies cannot add in an LV neutral wire and then couple to the transformer's MV winding, since the transformer would be an open circuit for zero sequence currents. To understand the origin of this switching frequency current, it was necessary to review the grounding scheme of the solar PV plant. This is shown in Fig. 16. This figure shows that in addition to the conductors carrying power at DC voltage from the solar panels, a conductor for grounding these panels is run to the skids. At the skid, the PV panel grounding conductor is bonded with conductors that ground various inverter components such as the inverter heat sinks, reactors and the inverter cabinet itself. These conductors are combined together and a single grounding conductor is then run to the transformer cabinet where it is bonded. The transformer cabinet is further bonded to the transformer neutral connection. The transformer cabinet is finally grounded by connecting it to the copper rod outside the skid i.e., the skid ground. In effect then, all the component grounds are interconnected and connected to the skid ground conductor.

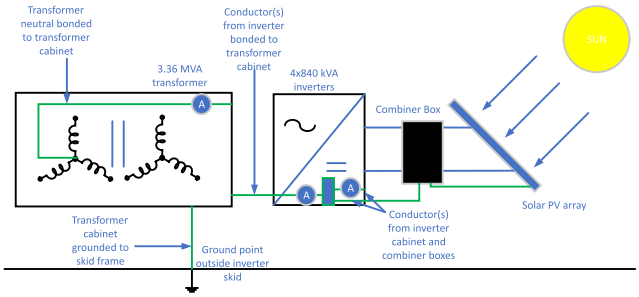

FIGURE 16. Schematic diagram of the grounding scheme of the PV plant.

The grounding scheme shown in Fig. 16 appears sound and follows standard practice. All the component grounds are interconnected under the assumption that they would carry current *only* under contingency conditions. Measurements of current in the inverter heat sink grounding conductor and the transformer neutral to ground conductor, however, showed that in this case this assumption was invalid. These measurements are shown in Fig. 17 and show that both these conductors, in fact, carry switching frequency currents. Further, since the source of the supraharmonics current is the switching of the power electronics in the inverter, it is reasonable to assume that the inverter heat sink grounding conductor may be the source of the supraharmonics current (notice that current magnitude from the inverter heat sink is also much higher in Fig. 17). It is also worth pointing out to the reader that other major components that carry switching frequency current inside the inverter cabinet, such as the inverter filter were being operated ungrounded in this case. Amongst the grounded inverter equipment, only the inverter heat sink had any direct connection to the switching frequency current.

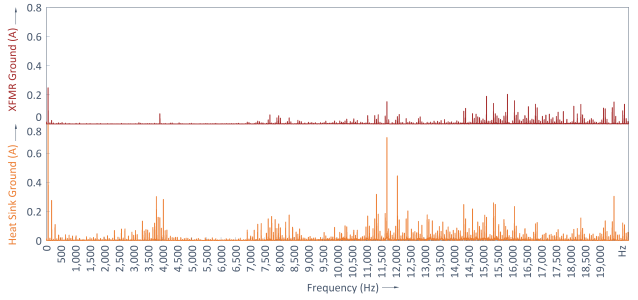

FIGURE 17. Spectrum of transformer ground current (top) and current in heat sink grounding conductor (bottom).

Confirmation of this hypothesis and an explanation for the presence of this switching frequency current in inverter grounding components is given in [17]. In this paper, the authors show that in power electronic circuits, a parasitic capacitance always exists between the power electronic switches and the heat sink to which they are mounted, which is typically grounded. This situation is shown in Fig. 18. The voltage differential that exists between power electronic switches, which are at line voltage and the grounded heat sink gives rise to the parasitic capacitance, and ultimately some current at the switching frequency constantly flows into this capacitance and ultimately the heat sink grounding conductor. In the situation shown in Fig. 16, the current in this parasitic capacitance couples with other conductors which are bonded to the heat sink grounding conductor. In the PV plant grounding scheme, since all grounding conductors are interconnected, the transformer neutral to ground conductors also carry this current which, in turn is carried in the concentric neutral conductor. Finally, since all the grounding conductors are bonded to the skid ground, the skid ground conductor offers a low impedance path to the switching frequency currents and also ends up carrying some of this current. This theory also logically and soundly explains the presence of switching frequency residue at 9 kHz at the solar panels. Since the grounding conductor for the solar panels and combiner boxes is also ultimately coupled to the other grounds at the skid, it also carries some of the current being leaked into the ground by the IGBT-heat sink parasitic capacitance. This current flows on the panel grounding conductor as it offers a low impedance path and was ultimately detected during the radiated emissions measurement (Fig. 10 and Fig. 11).

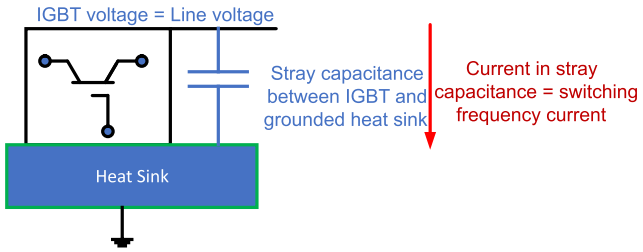

FIGURE 18. Single-line diagram showing stray capacitance between an IGBT switch and its heat sink.

V. DISCUSSION AND FUTURE WORK

The preceding sections have shown that the problem of audible noise described in this paper is rather unique and caused by a number of factors, all of which in of themselves would not otherwise cause this issue. In a nutshell, it can be described as a problem caused by a phenomenon of parasitic capacitance which seems to be well understood within the Power Electronics community but not so much within the PQ community. This phenomenon, coupled with grounding practice that is based on sound principles but applied without knowledge of the intricacies of solar PV emission, led to the background noise being observed. This discussion also highlights the need to revise standard grounding practice in the context of inverter based generation. Limited knowledge of supraharmonics emission within the Power Engineering community remains another limitation. Up to this point, conventional knowledge has been that supraharmonics are a localized phenomenon. However, the multi-point neutral grounded systems used in the United States can provide a low impedance path for such frequencies to propagate, if they do appear as common mode noise in some way. In the authors' experience, this noise is not necessarily restricted to solar

PV generation either. In fact the authors have seen another case in the US where a power electronics based reactive compensation device caused an identical problem on an MV feeder. Limited awareness of this phenomenon, however, has meant that standard grounding practice was not revised and reconsidered for devices which emit supraharmonics, leading to EMI with nearby telephone lines. It is hoped that this case will serve to inform PV system grounding practice (and grounding of other power electronically interfaced devices) and grid codes and raise awareness about potential problems due to parasitic capacitances with power electronic circuits in the future. It is proposed that this case study be put forward to bodies forming grid codes so that all aspects of PV inverter emission and grounding can be fully understood and existing practice be revised. Furthermore, to bridge the lack of standards regarding supraharmonics in the IEEE, it is proposed to include this case study into a white paper document about potential EMI problems that can result from suprharmonics. Ultimately the goal of such a white paper is to inform standards making and regulations on the subject of supraharmonics, and to inform PQ engineers of potential compatibility problems caused by such emission.

As a final note, it is worth discussing the mitigation solutions that have been tried by the utility for this problem so far. As previously discussed, the utility had considered inverter firmware changes to produce phase angle cancellation between a pair of inverters as a potential solution. While this solution met with success at two of the three affected sites, the broad emission spectrum produced by a different make and model of inverter meant that this solution had limited utility over a broader range of inverters. Next, the utility considered installing broadband filters to alleviate the problem of telephone interference. This solution, although predicted to reduce inverter common mode emission by 65%, has a number of problems. First, it has to be applied at every skid which is expensive. Secondly, this solution does not inherently solve the underlying problem but merely acts as a stop-gap. This prevents such problems recurring in the future. Finally, filters occupy space near the skid which can lead to problems with solar PV plants which have limited area. To permanently resolve the problem, the utility has considered disconnecting the concentric neutral conductor and the skid ground conductor from the distribution system neutral. However, this produces the problem of operating a distribution circuit without a ground reference. At the time of writing, the utility was looking at potential ways to isolate the solar PV plant neutral connection from the distribution system neutral. However, available solutions to accomplish this objective are typically not designed for the voltage levels being considered. The investigation into a possible solution, therefore, was ongoing at the time of writing.

REFERENCES

[1] S. Rönnberg and M. Bollen, "Power quality issues in the electric power system of the future," *Electr. J.*, vol. 29, no. 10, pp. 49–61, Dec. 2016. [Online]. Available: http://www.sciencedirect.com/science/article/pii/S1040619016302159

[2] *IEEE Standard for Harmonic Control in Electric Power Systems*, IEEE Standard 519–2022 (Revision IEEE Standard 519–2014), 2022, pp. 1–31.

[3] *EMC Limits for Harmonic Current Emissions (Equipment Input Current of 16A Per Phase)*, Standard 61000-3-2, 2014.

[4] S. K. Rönnberg, "Emission and interaction from domestic installations in the low voltage electricity network, up to 150 kHz," Ph.D. dissertation, Dept. Elect. Eng., Luleå Univ. Technol., Skellefteå, Sweden, 2013.

[5] S. K. Rönnberg et al., "On waveform distortion in the frequency range of 2 kHz–150 kHz—Review and research challenges," *Electr. Power Syst. Res.*, vol. 150, pp. 1–10, Sep. 2017. [Online]. Available: https://www.sciencedirect.com/science/article/pii/S0378779617301864

[6] A. Espín-Delgado, S. Rönnberg, and M. Bollen, "Uncertainties in the quantification of supraharmonic emission: Variations over time," in *Proc. Int. Conf. Renew. Energies Power Qual.*, 2020, pp. 1–6.

[7] Á. Espín-Delgado, S. Rönnberg, T. Busatto, V. Ravindran, and M. Bollen, "Summation law for supraharmonic currents (2–150 kHz) in low-voltage installations," *Electr. Power Syst. Res.*, vol. 184, Jul. 2020, Art. no. 106325. [Online]. Available: https://www.sciencedirect.com/science/article/pii/S0378779620301310

[8] *Assessment of Conducted Disturbances Above 2 kHz in MV and LV Power Systems*, CIGRE WG C4.31, Tech. Brochure 799, Apr. 2020.

[9] S. Schottke, S. Rademacher, J. Meyer, and P. Schegner, "Transfer characteristic of a MV/LV transformer in the frequency range between 2 kHz and 150 kHz," in *Proc. IEEE Int. Symp. Electromagn. Compat. (EMC)*, Aug. 2015, pp. 114–119.

[10] J. Behkesh Noshahr, "Emission phenomenon of supra-harmonics caused by switching of full-power frequency converter of wind turbines generator (PMSG) in smart grid," in *Proc. IEEE 16th Int. Conf. Environ. Electr. Eng. (EEEIC)*, Jun. 2016, pp. 1–6.

[11] A. M. Blanco, B. Heimbach, B. Wartmann, J. Meyer, M. Mangani, and M. Oeschger, "Harmonic, interharmonic and supraharmonic characterisation of a 12 MW wind park based on field measurements," *CIRED Open Access Proc. J.*, vol. 2017, no. 1, pp. 677–681, Oct. 2017. [Online]. Available: https://digital-library.theiet.org/content/journals/10.1049/oap-cired.2017.0457

[12] A. Mohos and J. Ladányi, "Emission measurement of a solar park in the frequency range of 2 to 150 kHz," in *Proc. Int. Symp. Electromagn. Compat. (EMC EUROPE)*, Aug. 2018, pp. 1024–1028.

[13] M. Mumtaz, S. I. Khan, W. A. Chaudhry, and Z. A. Khan, "Harmonic incursion at the point of common coupling due to small grid-connected power stations," *J. Electr. Syst. Inf. Technol.*, vol. 2, no. 3, pp. 368–377, Dec. 2015. [Online]. Available: https://www.sciencedirect.com/science/article/pii/S2314717215000550

[14] S. Sudha Letha, A. E. Delgado, S. K. Rönnberg, and M. H. J. Bollen, "Evaluation of medium voltage network for propagation of supraharmonics resonance," *Energies*, vol. 14, no. 4, p. 1093, Feb. 2021. [Online]. Available: https://www.mdpi.com/1996-1073/14/4/1093

[15] J. Sutaria, A. Espín-Delgado, and S. Rönnberg, "Supraharmonics within a datacenter-emission and propagation," in *Proc. 20th Int. Conf. Harmon. Quality Power (ICHQP)*, May 2022, pp. 1–6.

[16] G. Singh, E. Auel, J. Owens, T. Cooke, M. Stephens, and W. Howe, "Detection of high frequency conducted emission using radiated fields," in *Proc. IEEE PES Innov. Smart Grid Technol. Eur. (ISGT-Europe)*, Oct. 2020, pp. 334–338.

[17] F. Klotz, J. Petzoldt, and H. Volker, "Experimental and simulative investigations of conducted EMI performance of IGBTs for 5–10 kVA converters," in *Proc. PESC Record. 27th Annu. IEEE Power Electron. Spec. Conf.*, vol. 2, 1996, pp. 1986–1991.

GAURAV SINGH (Member, IEEE) received the master's and Ph.D. degree in electrical engineering from Clemson University, Clemson, SC, USA, in 2012 and 2017, respectively. He is currently with the Electric Power Research Institute, Knoxville, TN, USA, where he manages the program on transmission and distribution power quality. His research interests include harmonic and supraharmonic emission, compatibility issues created by power electronics-based loads and distributed energy resources, and development of new techniques for utilizing PQ data for incipient fault detection.

THOMAS COOKE (Member, IEEE) received the A.A.S. degree in electronics engineering technology from the Pellissippi State Technical Community College, Knoxville, TN, USA, and the B.S. degree in engineering technology and the M.S. degree in technology from East Tennessee State University. He is currently with the Electric Power Research Institute, Knoxville, where he manages the program on power quality data and monitoring. His research interests include the development of novel tools and techniques for power quality measurement, data visualization, and the application of machine learning for automatic waveform classification and analysis.

JASON JOHNS (Member, IEEE) received the A.A.S. degree in electrical engineering technology (EET) from the Pellissippi State Community College. He is currently pursuing the B.S. degree in electrical engineering with Arizona State University. He is also with the Electric Power Research Institute, Knoxville, TN, USA, where he manages the Knoxville Campus power quality monitoring service and conducts research in the field of novel power quality measurement tools and techniques. His research interests include PQ measurements and monitoring, PQ compatibility, and harmonic and supraharmonic emission.

LUIS VEGA (Member, IEEE) received the B.S. degree in mechanical engineering from Virginia Commonwealth University (VCU) and the M.B.A. degree from Averett University. He has been with Dominion Energy, Richmond, VA, USA, in a variety of roles for 22 years, with a focus on power quality for over a decade.

ARIEL VALDEZ (Member, IEEE) received the B.S. degree in electrical engineering from the Virginia Polytechnic Institute and State University (Virginia Tech) in 2008. He is a Licensed Professional Engineer in VA, USA. He is currently a Senior Engineer with Dominion Energy in distribution reliability. He has more than 15 years of power system experience in various engineering and operational roles. His current interests include distributed energy resource (DER) integration standards, and power quality and reliability.

GLORIA BULL (Member, IEEE) received the B.S. degree from the University of South Florida, Tampa, FL, USA, and the M.B.A. degree from Virginia Commonwealth University. She is currently the Supervisor of the Power Generation Electrical Engineering Team, Dominion Energy, Richmond, VA, USA. Prior to this role she worked as a project manager with the Renewable Energy Group, Dominion Energy.